

UDK: 539.375; 692.533.1; 546.261

Microstructure and Mechanical Properties of Aluminium Matrix Boron Carbide and Carbon Nanofiber Reinforced Hybrid Composites

Faik Okay^{1*}, Serkan Islak²

¹Department of Machine and Metal Technologies, Kastamonu Vocational High School, Kastamonu University, 37150, Kastamonu, Turkey

²Department of Mechanical Engineering, Faculty of Engineering and Architecture, Kastamonu University, 37150, Kastamonu, Turkey

Abstract:

In this study, aluminium matrix boron carbide (B_4C) and carbon nanofiber (CNF) reinforced hybrid composite was produced by powder metallurgy method and their microstructure and mechanical properties were investigated. The samples were produced at 6 percentage volume ratios using hot pressing technique. Microstructure examination, hardness measurement, transverse rupture test, and wear tests were carried out in order to determine the mechanical properties of the samples. Also three-point bending test was performed to determine their transverse rupture strength (TRS). Wear tests were carried out based on the ball on disc method. The microstructure examination revealed that the reinforcing elements were relatively homogeneously distributed in the aluminium matrix. In addition, the fracture was brittle due to the notch effect and agglomeration occurred with increasing amount of CNF. As the CNF amount of the samples increased, their hardness values increased but their TRS values decreased. Results of the wear test indicate that the increased amount of CNF increased the wear resistance. The friction coefficient values of the samples varied between 0.535 and 0.646. When the hardness was examined together with TRS and wear test results, the most suitable sample was determined to be Al-7%B₄C-1%CNF.

Keywords: Hybrid composites; CNF; Microstructure; TRS; Wear.

1. Introduction

The need for qualified materials is constantly increasing due to the ever-increasing energy price and the changes in the industry seen as a result of the developing technology,. In this context, scientists fabricate composite materials with very high performances by designing projects to produce novel and functional materials [1]. Current engineering applications require more robust, light-weight and cost-effective materials [2].

Metal matrix composites (MMCs) are mostly made of macro-scale mixture of reinforcing elements in the form of particle with the metal or alloy matrix [3]. Hybrid composites, on the other hand, are fabricated by adding more than one reinforcing element with different properties into the matrix [4]. Since MMCs are used in numerous areas such as the aerospace, automotive industry, defence, marine, and recreation industries, they have rapidly been replaced with traditional metallic alloys in many applications [5]. Metal carbides (SiC, TaC, WC and B₄C), metal nitrides (TaN, ZrN, Si₃N₄ and TiN), metal borides (TaB₂, ZrB₂, TiB₂ and WB), and metal oxides (ZrO₂, Al₂O₃, ThO₂ and SiO₂) are employed as the

*) Corresponding author: fokay@kastamonu.edu.tr

reinforcing elements in MMCs [3]. Aluminium is the most widely used metallic alloy as matrix material in the development of MMCs [6,7]. Aluminium matrix composites are used as structural members in automotive, aerospace, defence and marine applications because of its light weight, high strength to weight ratio, and excellent wear and corrosion resistance [8]. Fibre, whisker or particle reinforcements are added into the matrix based on the industrial needs. Aluminium matrix hybrid composites are new generation metal matrix composites that have the potential to meet recent demands of advanced engineering applications. They can meet such demands by means of their improved mechanical properties, adaptation to traditional processing technique, and their cost-effective production. The performance of aluminium matrix hybrid composites mostly depends on selection of the properly combined reinforcing elements [9].

Harichandran and Selvakumar [10] investigated the mechanical properties of nano and micron sized B_4C reinforced aluminium matrix composites. They used B_4C reinforcement at 2-10 % and stated that the ductility and tensile stress decreased at the reinforcement rates higher than 6 %. Results of the wear test indicated that the wear resistance increased up to 8 % B_4C reinforcement and then decreased with the increasing rate of reinforcement. Zhang et al., [11] examined the microstructure and mechanical properties of aluminium matrix composites with B_4C reinforcement at different volume fractions (5-10-15-20-25 %). They determined that the hardness increased with the increasing volume fraction of B_4C but the specific density of the composite decreased with the increasing volume fraction. The tensile test indicated that the ductility of the samples decreased with the increasing rate of B_4C reinforcement. They stated that the sample with volume fraction of 25 % had a very brittle structure. Baradeswaran et al., [12] investigated the microstructure and wear behaviour of aluminium matrix hybrid composites containing 10 wt% B_4C and 5 % graphite. They conducted the wear test using pin-on-disk device at different speeds and sliding speeds. They found that the wear rate increased with increased load but decreased with increased sliding speed. They determined that the decrease in wear rate was mainly associated with B_4C and graphite reinforcement. Oh et al., [13] examined the mechanical properties of aluminium matrix carbon nanofiber (CNF) reinforced composites. Copper (Cu) coated CNFs were added into the aluminium melt in order to wet them. In the study, CNF ranged between 0.065 wt% and 0.58 wt%. The microstructure examination revealed that the distribution was homogeneous. Upon examination of results of the tensile test, 0.58 % CNF reinforcement increased hardness by 131 % and tensile strength by 43.7 %. Lim et al., [14] investigated the effect of the distribution of CNF reinforcement in aluminium matrix composites on the mechanical properties. The surface of CNFs was coated with copper in order to increase the wettability of CNFs and prevent the formation of Al_3O_4 phase. They expressed that, after 1-minute mixture, the grain size of $10\mu m$ decreased to 2-5 μm in the production of CNFs. Yield strength and elastic modulus of the sample with 0.76 wt% CNF were greater by 33 % and 17 %, respectively compared to the non-reinforced sample.

The studies in the literature emphasized microstructure, mechanical and wear properties of MMCs produced with individual reinforcement of boron carbide and carbon nanofiber. However, the aim of the present study was to investigate the microstructure, mechanical and wear properties of the hybrid composites produced with the addition of both boron carbide and carbon nanofibers into the aluminium matrix. The hybrid composite, which is formed by adding CNF at very low volumes, has visibly improved main mechanical properties such as hardness, wear rate and friction coefficient.

2. Materials and Experimental Procedures

Al at 15-30 μm grain size, B_4C at average 10 μm grain size, and CNF with 100-nm diameter and 20-200 μm length were used as matrix materials to fabricate aluminium matrix

B₄C and CNF reinforced hybrid composites (Al-B₄C/CNF composite). The powders were mechanically alloyed at 200 rpm for 1 h. The ball-to-powder weight ratio was 10:1. The grinding media was steel balls, and the diameter was Φ 10mm. The mixed powders were produced using hot pressing method according to the volume fractions given in Table I at 550 °C and 35 MPa. The sizes of the samples were 40x10x10 mm.

Tab. I Composition of the samples.

Sample	Volume Fraction (%)		
	Al	B ₄ C	CNF
1	100	0	0
2	92	8	0
3	92	7.5	0.5
4	92	7	1
5	92	6.5	1.5
6	92	6	2

The Al-B₄C/CNF composite samples were subjected to the coarse and fine sanding stages and then they were polished using 1-micron diamond solution and etched using Keller solution. The relative and experimental densities of the samples were calculated. FEI QUANTA 250 FEG scanning electron microscope (SEM) was used to perform microstructure examination. In addition, XRD analysis was performed using Bruker D8 Advance brand X-ray device to determine the phase formation in the produced composite material. The hardness of the samples was measured in the Brinell hardness measurement device using 60 kg load and 1/8" diameter ball. Three-point bending test was performed in Shimadzu AG-IC model device to determine the transverse rupture strength of the samples. The wear test was made in UTS Tribometer T10/20 device in accordance with ASTM G133 standard.

3. Results and Discussion

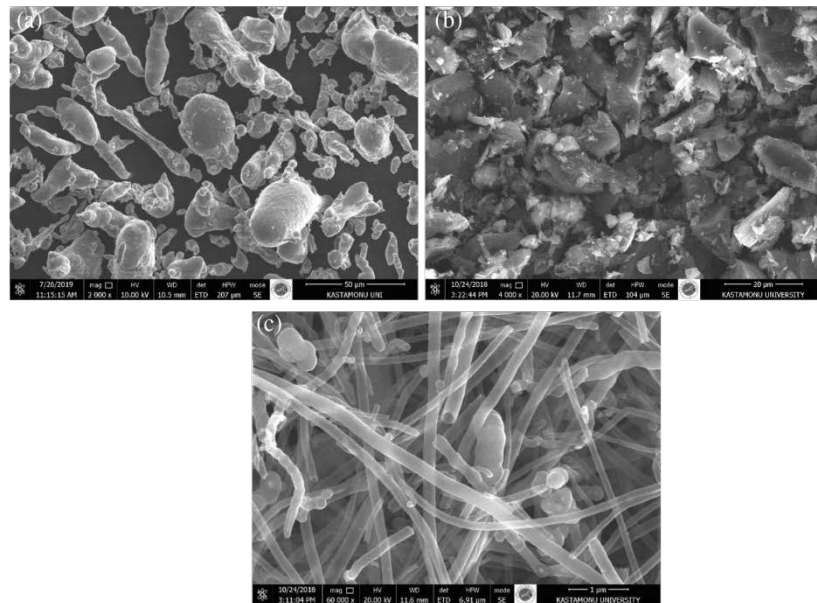


Fig. 1. SEM images of the powders used in the study (a) Al (b) B₄C (c) CNF.

Fig. 1 shows SEM images of the powders used in the production of Al-B₄C/CNF composite by hot pressing. Fig. 1 shows that while the aluminium powders have a relatively spherical and worm-like morphology. B₄Cs have a sharp-edge morphology. Also, CNFs have a fibrous morphology.

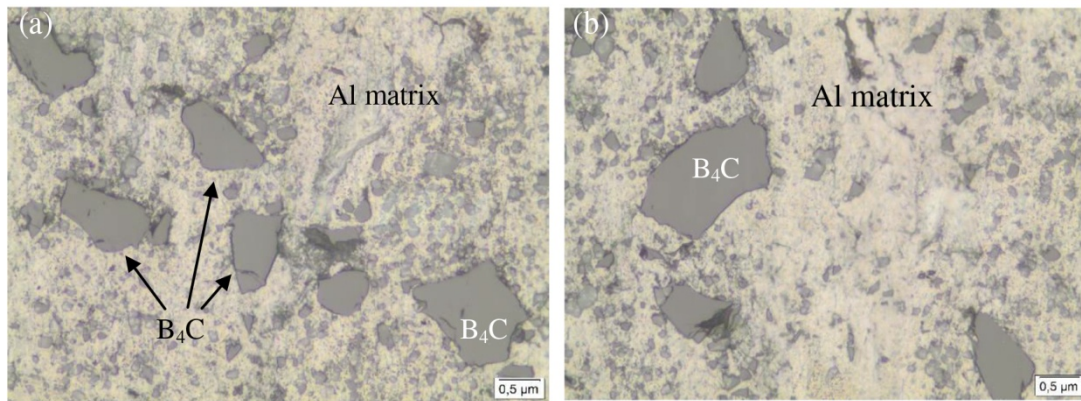


Fig. 2. Optical image of the samples (a) Sample 2 (8 % B₄C) 500x (b) Sample 3 (7.5 % B₄C + 0.5 % CNF).

Fig. 2 shows the optical images of the microstructure of Al-B₄C/CNF composite. B₄C grains are homogeneously distributed in the aluminium matrix. The reinforcement particles are embedded in the matrix interface.

Since the grain size of CNFs is smaller than the grain size of B₄C and aluminium matrix, CNFs are not clearly seen in optical images. Therefore, SEM images of the surfaces are also taken (Fig. 3). CNFs are embedded homogeneously in the aluminium matrix along with B₄C. Since the hybrid composite materials used in the study are produced by using powder metallurgy method, pores occur in the samples. It is considered that low grain size of CNFs reduces the pore amounts in the samples. SEM images clearly show this.



Fig. 3. SEM image of the surface of the sample 5.

X-Ray diffraction (XRD) analysis was conducted to determine the phases and compounds that may occur as a result of sintering of the Al-B₄C/CNF composite produced by hot pressing method. Fig. 4 shows XRD plots of all the samples.

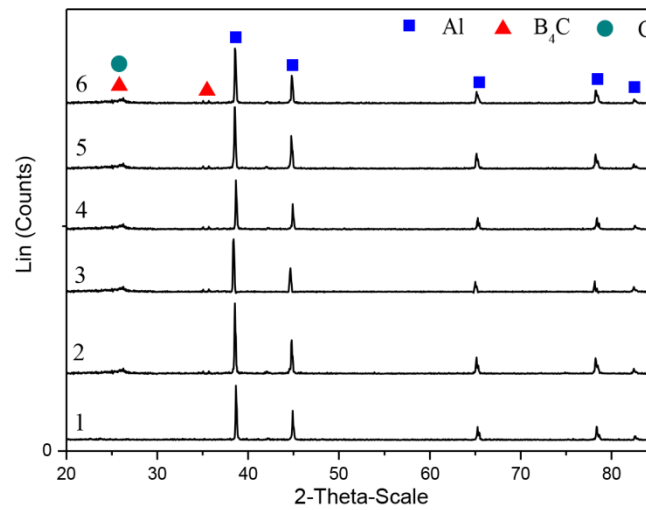


Fig. 4. XRD analysis of the samples.

Only the aluminium peak is seen in the non-reinforced sample 1 (Fig. 4). This is normal since there is no reinforcement in the sample 1. Bragg angle values of aluminium are 38.653° ; 44.898° ; 65.248° ; 78.352° , and 82.602° . While Bragg angles for B₄C are 23.393° and 37.691° , Bragg angle for C is 26.304° . Phase C represents CNF. In addition, separate XRD analysis is performed for the region where the bragg angle is 20-38 degrees where there are no aluminium peaks (Fig. 5). Upon examination of the other samples it is seen that B₄C and C peaks form and there are increases in the intensities of these peaks with increasing reinforcement rate. No new phase forms in the structure. It is also understood from XRD analysis that there is no oxide formation in the structure.

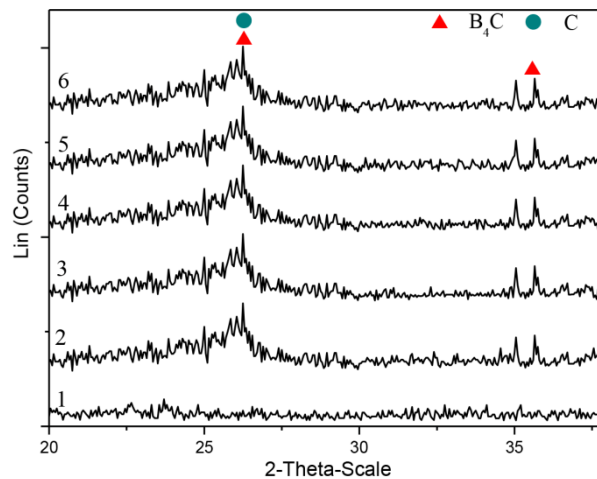


Fig. 5. XRD analysis of the samples with Bragg angle from 20 to 38.

Density measurement was conducted to determine the effect of change in the reinforcement rate of Al-B₄C/CNF composite on the density of the produced composite. Density measurements were measured on the basis of Archimedes principle. 0.1 mg precision scales were used in density measurement. First, samples were weighed in the air, immersed in a container filled with distilled water, and weighed again. The experimental densities of the

samples vary between 2.582 and 2.680 g/cm³, the theoretical density is 2.673 – 2.700 g/cm³ and corresponding relative density varies between 96.6 and 99.2 % (Table II).

Tab. II Density values of the samples.

Samples	Theoretical Density (g/cm ³)	Experimental Density (g/cm ³)	Relative Density (%)
1	2,700	2,680	99,2
2	2,685	2,644	98,4
3	2,682	2,631	98,1
4	2,679	2,602	97,1
5	2,676	2,589	96,7
6	2,673	2,582	96,6

Based on the relative densities of the samples, the density of the composite decreases as the amount of KNF increases (Fig. 6). This decrease may be associated with the aluminium density of 2.7 g/cm³, B₄C density of 2.52 g/cm³ and CNF density of 1.9 g/cm³. Considering the other components, as the CNF amount with low density increases, the relative density decreases. In a similar study, Islak [15] states that density decreases as the reinforcement rate in the produced composite material increases. In their study, Rahimian et al., [16] explain that the increase in the reinforcement rate at constant sintering temperature negatively affects the compressibility and in this case, it decreases the relative density. The reason why the relative densities are close to each other in this study (96.6-99.2 %) can be suitable sintering parameters under hot pressing conditions. Since the diffusion rate between powder particles increases due to sintering process, the experimental densities are close to each other, which affects the relative density. Lima et al., [17] explain that the increasing temperature in sintering process increases the formation of solid bond between particles and accelerates the diffusion of particles to each other.

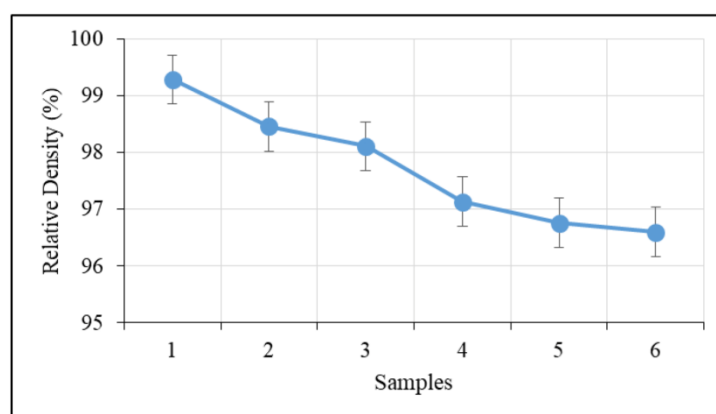


Fig. 6. Relative density change of the composite material.

The hardness of the samples is measured in a Brinell Hardness Measurement device using 60 kg load and 1/8'' diameter ball. Fig. 6 shows Brinell hardness values (HB). Based on the Fig. 6, the hardness of the sample 1 (containing pure Al) is 75 HB and the hardness of the other reinforced samples is between 80 and 90 HB. It can be asserted that as the rate of CNF increases, the hardness increases. The hardness of the sample 6 (2 % CNF), is 90 HB. It is

known that hardness values generally increase as the rate of reinforcing element in aluminium matrix composite material increases. This is explained by Islak [15] based on mixing rule. Equation 1 shows this mixing rule.

$$H_k = H_m f_m + H_r f_r \quad (1)$$

where H_k refers to the hardness of the composite, H_m and H_r refer to the hardness of matrix and reinforcement, respectively. Also, f_m and f_r refer to the volumetric rates of matrix and reinforcing element [18]. Since the hardness of the reinforcing element is higher than the hardness of the matrix material, the hardness of the composite material would be higher than the hardness of the matrix material depending on the volume fraction.

The three-point bending test is conducted with the samples of 40x10x10 mm dimensions and at 0.5 mm/min test speed in order to determine the transverse rupture strength of Al-B₄C/CNF composite. The effect of reinforcing element on the transverse rupture strength (TRS) of the composites is investigated. The TRS values of the composites are measured as 103-90-72-68-56-53 MPa (Fig. 6). As the CNF reinforcement increases, the TRS values decreases.

There is a negative correlation between the hardness and TRS values of the samples (Fig. 7). Although the volume fraction of reinforcement is kept constant in the study, the effect of CNF is high in the composite since the specific weight of CNF is lower than the specific weight of B₄C. The decrease in the relative density of the samples causes a decrease in the TRS values. Islak [15] reveals that the increase in the reinforcement rate leads the cross section to weaken, thus resulting in decreased TRS values. In addition, Pul [19] states that the increase in reinforcement rate forms a notch effect and decreases the TRS values of the material.

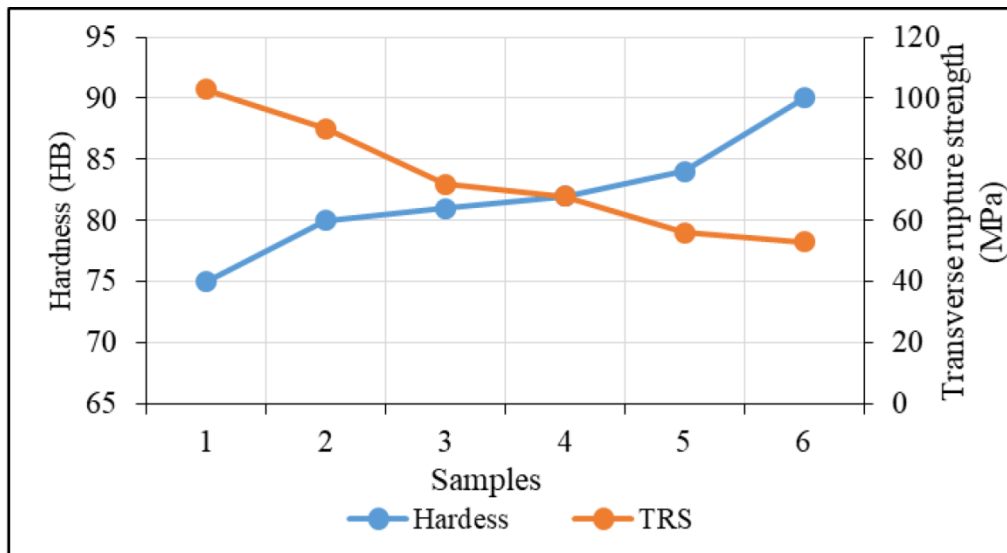


Fig. 7. Comparison of hardness and transverse rupture strength of the samples.

The SEM images taken from the fracture surfaces of the samples subjected to three-point bending test are examined (Fig. 8). Small grain size causes B₄C to be positioned in the gaps in the matrix and thus the reinforcing element is homogeneously distributed in the matrix. The fracture form in the Sample 2 without KNF is brittle. Brittle fracture occurs by creating a notch effect in boron carbide grains.

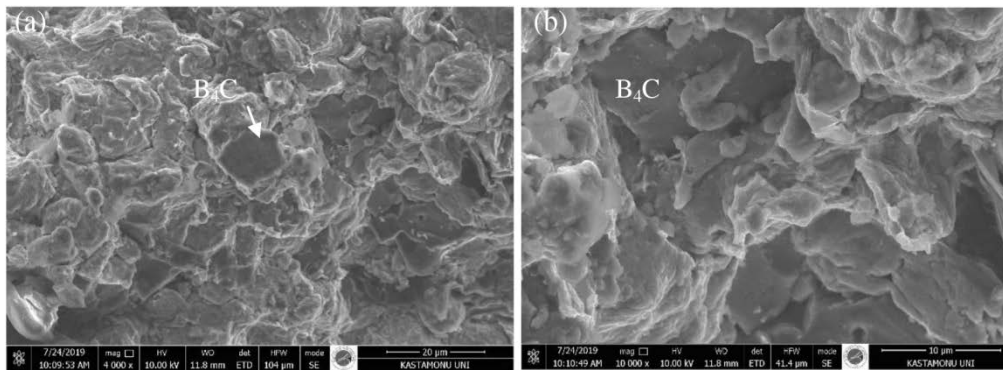


Fig. 8. SEM image of the fracture surface of the sample 2 (a) 4000x (b) 10000x.

SEM image of the sample 6 (6 % B_4C + 2 % CNF) shows that the fracture shape in fracture surface is in the form of separating from the grains (Fig. 9). Even a small number pores form in the structure. Also, the grains have waisting due to sintering.

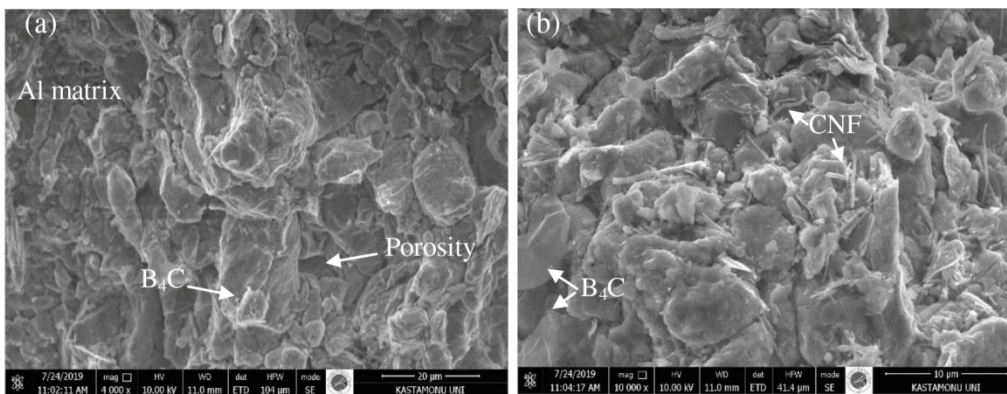


Fig. 9. SEM image of the fracture surface of the sample 6 (a) 4000x (b) 10000x.

SEM image of the sample 5 (6.5 % B_4C + 1.5 % CNF) shows that B_4C s are homogeneously distributed in the matrix. B_4C grains are firmly attached within the matrix. However, agglomeration occur in some places as the rate of CNF increases (Fig. 10).

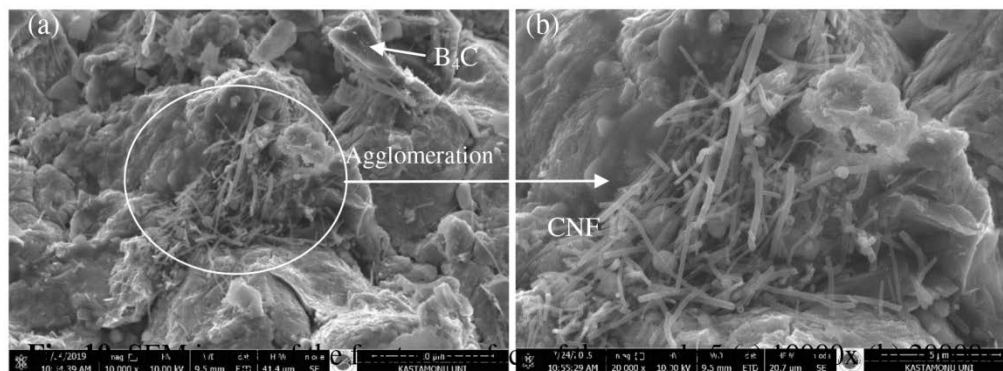


Fig. 10. SEM image of the fracture surface of the sample 5 (a) 10000x (b) 20000x.

SEM images of the fracture surfaces of the samples show that the fractures are mostly composed of the matrix and reinforcing element interface. Since reinforcing element B_4C and CNF are harder than aluminium matrix, it causes a notch effect in the composite structure. In addition, this is associated with wetting problem, namely matrix material couldn't adequately wet the reinforcing element. Based on Fig. 11, CNFs are broken and shorten in three-point bending test. The fracture is brittle in general. In the study, it is considered that this brittle fracture is associated with the fact that TRS values decrease with increasing rate of CNF. The TRS values of the samples decrease from 103 MPa to 53 MPa. Günay [20] explains that this decrease is associated with the pore/lubricant density causing a decrease in the density of composite material with increasing reinforcement rate.

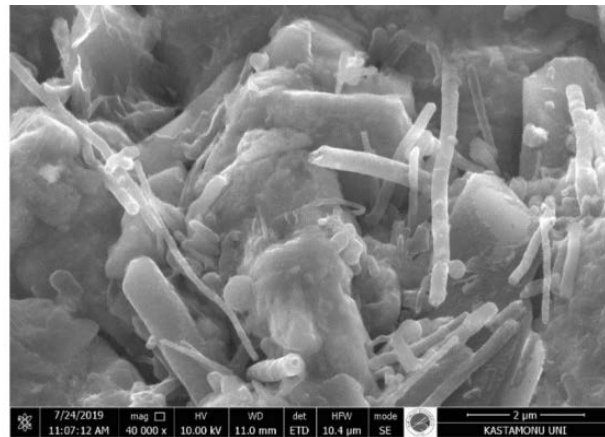


Fig. 11. SEM image of the fracture surface of the sample 6, 40000x.

In order to determine the wear resistance of the Al- B_4C /CNF composite, reciprocating wear test is performed in accordance with ASTM G133 standards under 5 N load at 200 m sliding distance and 0.06 m/s test speed. The abrasion test is carried out using 52100 quality steel ball with 5-mm diameter at normal atmospheric temperature and in a dry environment. The parameters in the wear test are determined in accordance with the other studies. In their study, Mindivan and Kayalı [21] perform the wear test of aluminium matrix SiC reinforced composites at a load of 1.5-6 N and a sliding speed of 0.02 – 0.09 m/s. As a result of the wear test result of the hybrid composite material, the wear rate and friction coefficient values are present in Fig. 12.

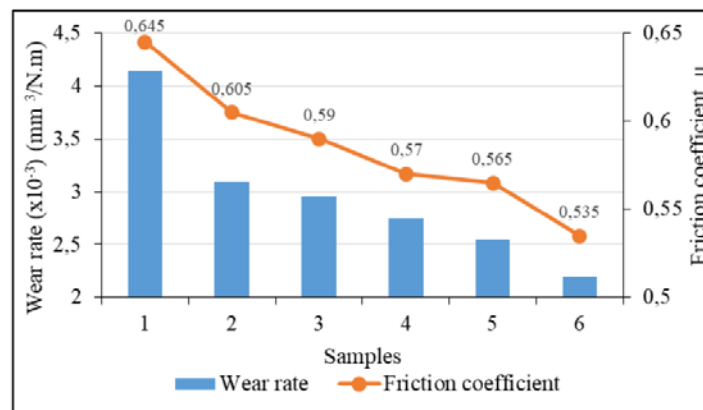


Fig. 12. The wear rate and friction coefficient values of the samples.

As a result of the wear test of the samples, the friction coefficient values vary between 0.645 and 0.535. The friction coefficient is 0.645 in the sample 1 containing matrix material. The friction coefficient of sample 6, which has the highest hardness, is measured as 0.535. As the rate of CNF in the samples increases, the friction coefficient also decreases. Ramesh et al., [22] reports that the friction coefficient decreases with increasing rate of carbon fibre reinforcement. In their study, Mindivan and Kayalı [20] reveal that the friction coefficients under 3 and 4.5 N test load vary between 0.5 and 1.

Based on the wear rates of the samples, it can be asserted that the wear resistance also increases with increasing hardness [23]. As the hardness values of the samples increase, the wear rate decreases (Fig. 13). The wear rate of the sample 1 is $4.13 \times 10^{-3} \text{ mm}^3/\text{Nm}$ and the wear amount of the sample 6 is $2.20 \times 10^{-3} \text{ mm}^3/\text{Nm}$. Hasırcı and Gül [24] investigate the effect of reinforcement volume fraction of B_4C reinforced aluminium matrix composites on the abrasive wear and reveal that as the hardness of the samples increases, the wear resistance also increases.

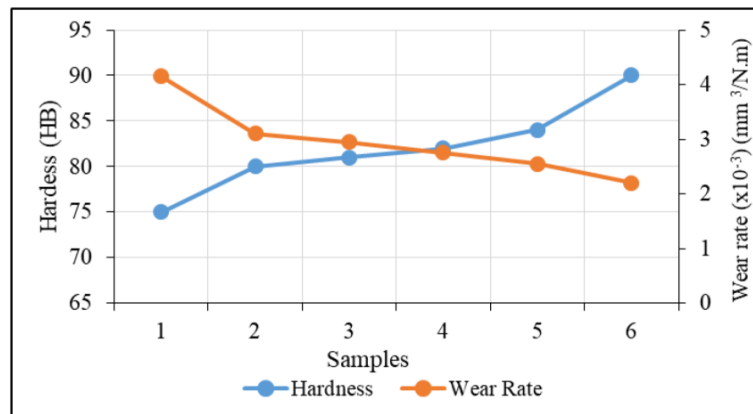


Fig. 13. Comparison of hardness-wear ratio of the samples.

SEM images for the wear surfaces of the samples are examined. Fig. 14 shows surface image of the unreinforced sample. Adhesive and abrasive wear mechanisms occur. Fig. 14 clearly shows the traces in the direction of slide forming during the wear test (a). In the unreinforced sample, wear zones in the form of wide grooves in the sliding direction are seen (Fig. 12 (b)). Adhesive wear mechanism is dominant in the unreinforced sample caused by ruptures from the surface depending on very high plastic deformation.

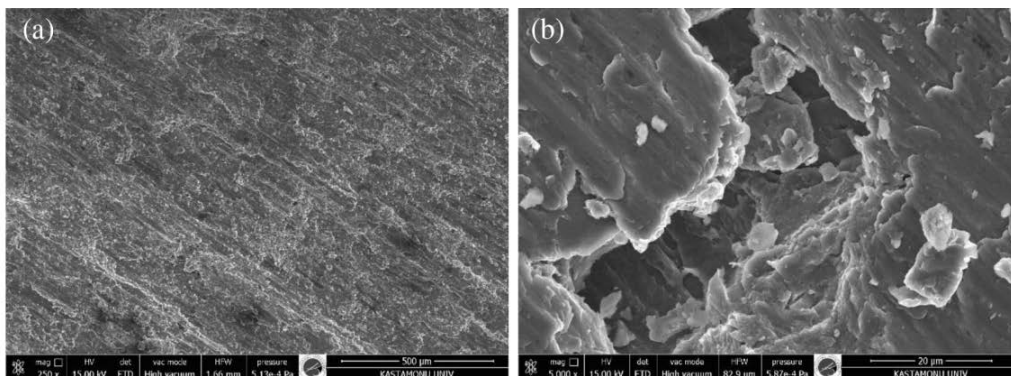


Fig. 14. SEM image of the wear surface of the unreinforced sample (a) 250x (b) 5000x.

Fig. 15 shows the image of wear surface of the sample 2 with 8 % B_4C reinforcement. Traces in the sliding direction are seen. In addition, the reinforcing element retains on the surface.

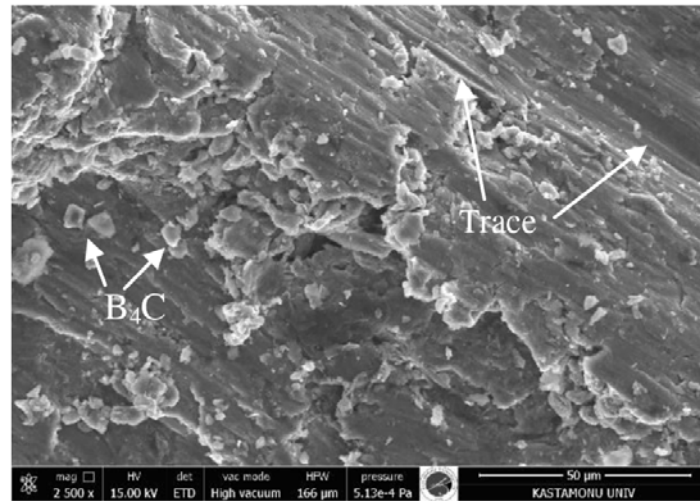


Fig. 15. SEM image of the wear surface of the sample 2, 2500x.

Fig. 16 shows wear surface images of the samples 4 and 6. The traces in the sliding direction are seen. The abrasive wear mechanism is generally dominant in the reinforced samples. The hardness of the sample increases due to effect of the reinforcement and the plastic deformation on the sample surface decreases with the increasing hardness. As hardness in the samples increases, their abrasion rate also decreases. Wear surface images also confirm this result. As the CNF rate of the samples increased, traces on the surface decrease.

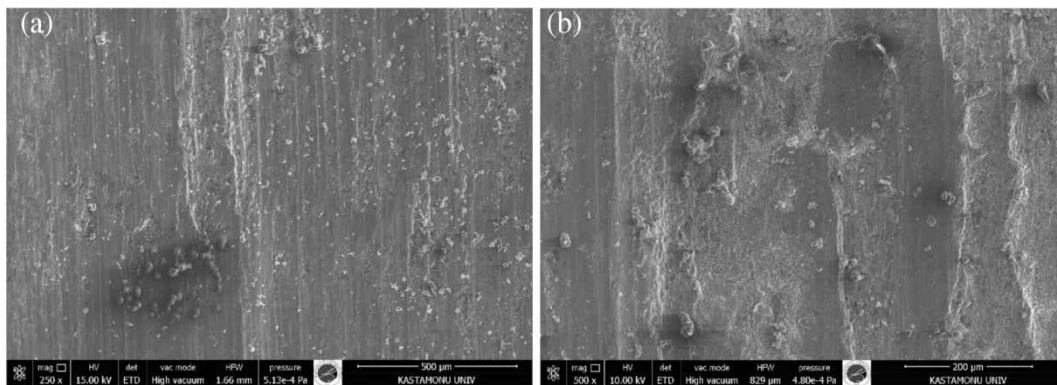


Fig. 16. SEM image of the wear surface of the samples 4 and 6 (a) 250x (b) 500x.

Fig. 17 shows image of the wear surface of the sample 6 and the EDS analysis taken from various points and regions of the sample. EDS analysis also supported the analysis in SEM images. In the analyses, the presence of oxygen along with the matrix and reinforcing element is determined. During the wear test, oxide layer forms even partially depending on the increasing temperature on the surface.

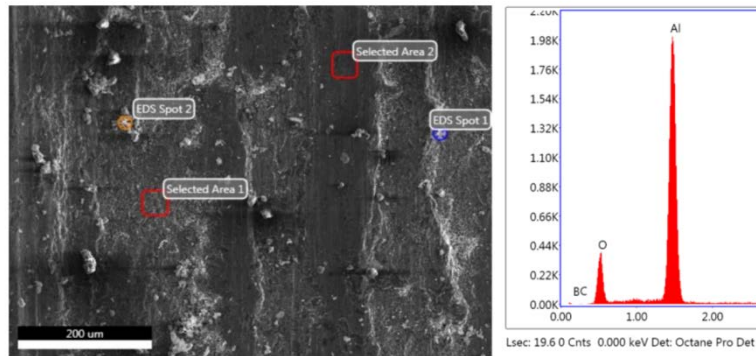


Fig. 17. EDS analysis of the wear surface of the sample 6 (Area 2).

Table III shows summary of mechanical properties including the results of the experiments.

Tab. III Mechanical properties of the Al-B₄C/CNF.

Samples	Hardness (HBN)	TRS values (MPa)	Relative Density (%)	Wear Rate ($\times 10^{-3}$) (mm ³ /Nm)	Friction Coefficient (μ)
1	75	103	99,2	4,15	0,645
2	80	90	98,4	3,10	0,605
3	81	72	98,1	2,95	0,59
4	82	68	97,1	2,75	0,57
5	84	56	96,7	2,55	0,565
6	90	53	96,6	2,20	0,535

With the increasing rate of CNF, hardness values increase and TRS values decrease. Relative density decreases, wear properties improve and friction coefficient decreases. In other words, we can evaluate that there is a noticeable improvement in mechanical properties with increasing rate of CNF.

4. Conclusion

In this study aiming to investigate the microstructure and mechanical properties of Al-B₄C/CNF composite, the following results were obtained:

1. In SEM studies, B₄C and CNF reinforcements in the aluminium matrix were relatively homogeneously distributed in the aluminium matrix. XRD analysis showed that no intermediate phase formed in the produced hybrid composite material. In addition, no oxide formation occurred.
2. The relative density values of the samples varied between 99.2 and 96.6 %. Relative density values decreased as CNF reinforcement increased. In the sample 6 with 2 % CNF, the lowest relative density was measured as 96.6 %.
3. With the increased CNF reinforcements in the samples, the hardness values increased. While the mean hardness value was measured as 75 HB in the unreinforced sample 1,

the hardness was measured as 81 HB in the sample with 1 % CNF and 90 HB in the sample with 2 % CNF.

4. As a result of the three-point bending test, the highest TRS value was measured as 103 MPa in the sample 1. The lowest TRS value was obtained in the sample 6 with the highest sample hardness and the TRS value was found as 53 MPa. TRS values of the samples decreased with the increased rate of CNF reinforcement. The shape of fracture was separation between grains in general. The increase rate of CNF reinforcement caused a little agglomeration. The fractures in fibres used were brittle.
5. Results of wear test showed that with increasing rate of CNF, wear rates and coefficients of friction decreased. The lowest wear rate and coefficient of friction were determined in the sample 6 hybrid composite.

5. References

1. R. Y. Lin, K. Kannikeswaran, In *Interfaces in Metal-Ceramic Composites*, (1990) 153.
2. S. C. Tjong, In *Nanocrystalline Materials*, Elsevier Press, (2014) (English)
3. J. W. Kaczmar, K. Pietrzak, W. Włosiński, *Journal of materials processing technology*, 106 (1-3) (2000) 58.
4. J. D. Torralba, C. E. Da Costa, F. Velasco, *Journal of Materials Processing Technology*, 133(1-2) (2003) 203.
5. D. K. Das, P. C. Mishra, S. Singh, S. Pattanaik, *International Journal of Mechanical and Materials Engineering*, 9 (1) (2014) 6.
6. B. S. Yigezu, M. M. Mahapatra, P. K. Jha, *Journal of Minerals and Materials Characterization and Engineering*, 1 (4) (2013) 7.
7. C. Padmavathi, A. Upadhyaya, *Science of Sintering*, 42 (3) (2010) 363.
8. Y. Kaplan, S. Aksöz, H. Ada, E. İnci, S. Özsoy, *Science of Sintering*, 52(4) (2020) 445.
9. M. O. Bodunrin, K. K. Alaneme, L. H. Chown, *Journal of materials research and technology*, 4 (4) (2015) 434.
10. R. Harichandran, N. Selvakumar, *Archives of Civil and Mechanical Engineering*, 16 (1) (2016) 147.
11. L. Zhang, Z. Wang, Q. Li, J. Wu, G. Shi, F. Qi, X. Zhou, *Ceramics International*, 44 (3) (2018) 3048.
12. A. Baradeswaran, S. C. Vettivel, A. E. Perumal, N. Selvakumar, R. F. Issac, *Materials & Design*, 63 (2014) 620.
13. S. I. Oh, J. Y. Lim, Y. C. Kim, J. Yoon, G. H. Kim, J. Lee, J. H. Han, *Journal of Alloys and Compounds*, 542 (2012) 111.
14. J. Y. Lim, S. I. Oh, Y. C. Kim, K. K. Jee, Y. M. Sung, J. H. Han, *Materials Science and Engineering: A*, 556 (2012) 337.
15. S. Islak, *Science of Sintering*, 51(1) (2019) 81.
16. M. Rahimian, N. Ehsani, N. Parvin, H. reza Baharvandi, *Journal of Materials Processing Technology*, 209 (14) (2009) 5387
17. W. M. Lima, F. J. Velasco, J. Abenojar, J. M. Torralba, *Journal of materials processing technology*, 143 (2003) 698.
18. S. Yang, Z. Guo, M. Xia, *Science of Sintering*, 50(2) (2018) 237.
19. M. Pul, *International Journal of Engineering Research and Development*, 11(1) (2019) 87.
20. M. Günay, U. Şeker, *Materials Science Forum*, 672 (2011) 319.
21. H. Mindivan, E. S. Kayalı, *İTÜDERGİSİ/d*, 6(2) (2010) 63.
22. C. S. Ramesh, H. Adarsha, S. Pramod, Z. Khan, *Materials & Design*, 50 (2013) 597.

23. M. Pul, Science of Sintering, 50(1) (2018) 51.
24. H. Hasırcı, F. Gül, SDU International Technologic Science, 2 (1) (2010) 15.

Сажетак: У овом раду су испитивана микроструктура и механичка својства бор карбида (B_4C) и хибридног композита ојачаног карбонским нановлакнима (CNF) добијених методом металургије праха. Узорци су добијени топлим пресовањем. Спроведена су микроструктурна испитивања, мерења тврдоће, тест попречног лома и хабања да би се одредила механичка својства узорака. Такође, савијање у три тачке је урађено да би се одредила чврстоћа попречног кидања (TRS). Тест на хабање је изведен на бази лопте на диску. Микроструктурна испитивања су открила да су елементи ојачања били релативно хомогено распоређена у матрици алуминијума. Прелом је био крт услед ефекта зареза и агломерације која се појавила са повећањем количине CNF. Како је количина CNF у узорку расла, вредности тврдоће су расле, али је TRS опадао. Резултати теста хабања указују да повећана количина CNF утиче на раст отпорности на хабање. Коефицијент фриксије је варирао између 0.535 и 0.646. Када је тврдоћа испитивана заједно са TRS и хабањем, најстабилнији узорак је био састава $Al-7%B_4C-1\%CNF$.

Кључне речи: хибридни композити, CNF, микроструктура, TRS, хабање.

© 2022 Authors. Published by association for ETRAN Society. This article is an open access article distributed under the terms and conditions of the Creative Commons — Attribution 4.0 International license (<https://creativecommons.org/licenses/by/4.0/>).

